

The Northern Central Indian Ridge: Geology and tectonics of fracture zones-dominated spreading ridge segments

R. K. Drolia*, Sridhar D. Iyer[†], B. Chakraborty, V. N. Kodagali, D. Ray, S. Misra[‡], R. Andrade*, K. V. L. N. S. Sarma[§], R. P. Rajasekhar* and Ranadhir Mukhopadhyay**

National Institute of Oceanography, Dona Paula, Goa 403 004, India

*National Geophysical Research Institute, Uppal Road, Hyderabad 500 007, India

[‡]Department of Geology and Geophysics, Indian Institute of Technology, Kharagpur 721 302, India

[§]National Institute of Oceanography, 176, Lawsons Bay Colony, Visakhapatnam 530 001, India

**Present address: Mauritius Oceanography Institute, France Centre, Quatre Bornes, Mauritius

Multi-beam and single-beam bathymetric, gravity and magnetic data, across seven ridge segments (length varying between 37 and 84 km), offset by six transform discontinuities (ranging in dislocation length between 48 and 344 km) of the Northern Central Indian Ridge (NCIR) were collected. Four Transform Faults (TF, viz. Sealark, Vityaz, Ehrlich and Vema) have been mapped in detail; while studies on geological, biological and water sampling were carried out at the last three transform faults. The ridge segments are characterized by along-axis depth variation: deepening at segment ends and shallowing at the centre. Both the ridge axis and TF areas are complex with intra- and inter-segmental morphotectonic and magnetic variations. Basalts collected from axial valley, Ridge-Transform Intersection (RTI) and from near-axis seamount, exhibit pillow and columnar structures. Samples from the RTI yielded ferromanganese crust, nodules and intensely bioturbated calcareous sediments hosting nannoplanktons. The characteristics of the RTI, axial valley and transform and the presence of neo-volcanic zones along ridge-normal profiles suggest predominance of tectonomagmatic activities in the Vityaz and Vema regions. In the Sealark region, tectonic activities dominate.

THE Central Indian Ridge (CIR), spreading at a half spreading rate of 20–30 mm/yr, is a part of the 70,000 km long global Mid-Ocean Ridges (MOR) and constitutes an important regime of divergent plate boundaries. In terms of structural fabric, spreading kinematics and isotope geochemistry of the erupted lava, this region differs strikingly from the MOR in the other oceans. The Northern Central Indian Ridge (NCIR; 18 to 21 mm/yr) spans from 2°S to 12°S and encompasses the accreting plate boundaries between Australia and Africa in the south, and India and Africa in the north. The zone of intersection between

the CIR and the Diffused Deformation Zone (DDZ) separates these two plate boundaries (Figure 1). The DDZ is

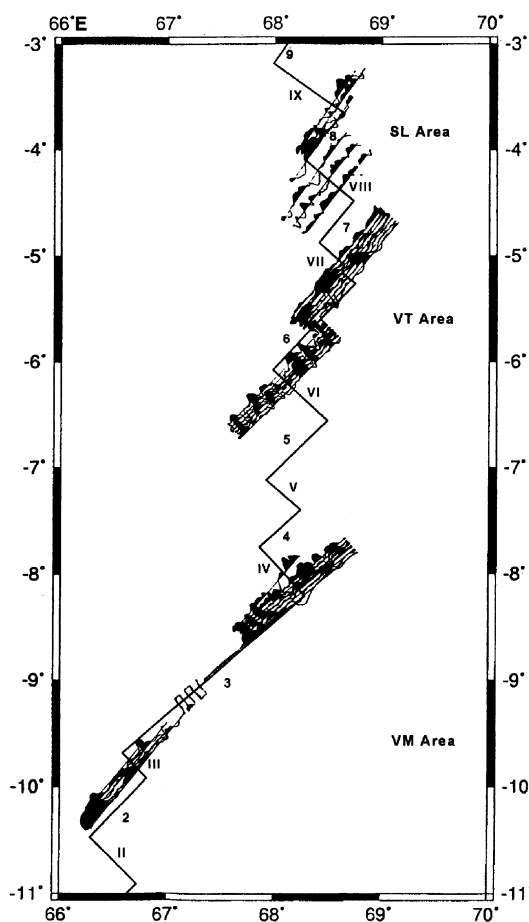


Figure 1. Location of the Sealark (SL), Vityaz (VT) and Vema (VM) transform faults. The ridge segments are shown as NW-SE oriented double lines while the transform faults are depicted as NE-SW trending solid black lines. The axial ridge segments and the transform segments are numbered in Roman and numerical style, respectively. Magnetic anomalies are plotted perpendicular to cruise tracks.

[†]For correspondence. (e-mail: iyer@csnio.ren.nic.in)

20–18 Ma old and runs along the equator from the CIR in the west to the Wharton Basin in the east and separates the Indian and Australian plates. Hence, the intersection of DDZ with the CIR between 4°S and 8°S should potentially initiate the formation of a triple junction of Indo-Australian and African plates.

The geophysical details available for the entire CIR system pertain to satellite gravity and magnetic data^{1,2}, the interpretation from few magnetic lines in the Vema transform fault (TF) area^{3–5} and the tectonic implications of bathymetric and magnetic data of the Vema TF^{6,7}, while the rocks recovered from disparate areas were also reported^{8–10}. However, there is no multi-beam swath bathymetry data available from the region between 2° and 12°S except for some reconnaissance survey made in 1983 during the 28th cruise of F/S Sonne¹¹. Furthermore, in the absence of any significant data from Vityaz and Sealark TF areas, the influence of Ridge-Transform Intersections (RTI) on plate geometry and the formation of a nascent triple junction was incomplete.

The complex structural features and magmatic processes along the CIR not only constrain the formation of the new crust, but also play a major role in biogeochemistry, petrology, geochemical and thermal evolution and the circulation of hydrothermal fluid along this ridge. But the exact nature of the dynamics and reasons thereof are unclear, primarily due to lack of supporting real time data of the seafloor and in-depth studies. An effort to plug this gap in knowledge was initiated in 1997, under the project 'Tectonics and petrological implications of fracture zones on crustal generation along the Central Indian Ridge' (a project under the InRidge programme of India), to focus on the crustal fabric at the intersection between the axial ridge and the TF, petrological variations in response to ridge segmentation, relation of fracture zones (FZ) to hotspots and axial seamounts and role of morphotectonics on hydrothermal circulation.

In consideration and continuation to the findings from previous studies, particularly from the first expedition (July–August 1997; *ORV Sagar Kanya*, SK #125), a second cruise (ORVSK #165) was undertaken during May to July 2001. During the cruise, the geological and geophysical signatures at the intersection of the CIR with the DDZ (4°S and 8°S) were investigated. Also examined were RTI characteristics of the areas between three major FZ (Sealark-SL, Vityaz-VT, and Vema-VM; Figure 1). Sampling at several sites was carried out along the FZ, ridge segments and near-axis seamounts.

Data acquisition and processing

The expedition involved collection of under-way geophysical data, viz. multi-beam and single-beam bathymetry, gravity and magnetic as well as rocks, sediment, water, and biological samples. High quality multi-beam

swath bathymetric, gravity and magnetic data over three intersecting regions of SL FZ-NCIR (SL area), VT FZ-NCIR (VT area) and VM FZ-NCIR (VM area) were acquired along 53 ridge-normal profiles covering lengths between 125 and 200 km across seven ridge segments¹³. The profiles across the ridge segments extend up to a length of 148 km (111 km in profiles of SL area) on either side of the axial valley. This is probably the first time that such an extensive geophysical mapping was made at closely spaced profiles (2 nm interval) across ridge axis in proximity to the RTI. In all, 5498 km each of gravity and multi-beam bathymetry, 4941 km of magnetic and 5827 km of single-beam bathymetry data were collected and manually recorded at 10 min interval in specific data sheets.

Under-way data were collected through a Bodensee-work Sea Gravimeter System (KSS 30), a Geometrics Proton magnetometer (G-801/3) and a Honeywell-Elac Deep Sea wide beam echo sounder. Swath mapping of the seafloor with 100% coverage was achieved through the Multibeam-Hydrosweep system (STN Atlas Elektronik GmbH, Germany). The system operates at 15.5 kHz and makes use of 59 Pre-Formed Beams with an average beam width of 2.3°. This configuration results in a swath coverage of twice the water depth in the area. An inter-line (i.e. the distance between two profiles) spacing of 2 nm (nautical mile) was maintained (except for six profiles in VM area) to obtain 100% coverage (insonification) of the sea floor.

Acoustic Doppler Current Profiler (ADCP) data and biological samples at two stations were collected from the surface and subsurface depth up to 500 m. This first effort was made to initiate the process of resolving the coupling between biological and oceanographic processes. The method involves the ability to gather biological data at the same spatial and temporal rates as other environmental variables, as these are key factors to decipher the dynamics of marine ecosystems. Such a study also helps to understand the role of biology in modifying climate via air–sea flux of carbon dioxide. Nine chain bag dredge operations were carried out at the RTI and from near-axis seamounts in VM and VT areas, with recovery in two instances. The details of the various sampling operations are given in Table 1.

Post-cruise data processing involved digitization of echograms and interpolation of magnetic data at 1 min interval, merging the magnetic field intensity data with bathymetry and applying the Mathew's correction to obtain the corrected depth. The magnetic anomaly was computed by subtracting IGRF 2000 from the observed interpolated total intensity data. We have used the revised ridge-transform geometry of the NCIR based on latest satellite-derived gravity map¹. To facilitate the discussion of the accretionary units, the ridge segments (from south to north) are numbered as I to IX and the TF/FZ as 1 to 9 (Figure 1).

The magnetic profiles were plotted perpendicular to the ship tracks and projected onto the ridge normal direction (Figure 1). Considering an average spreading rate of 18 mm/yr, a magnetized layer thickness of 500 m and susceptibility contrast of 0.01 c.g.s. units and based on the reversal time-scale¹², we have modelled the observed profiles and identified the anomalies. Multi-beam swath bathymetric data were processed to obtain bathymetric maps of the three surveyed regions (Figure 2). Single-beam bathymetric profiles have been drawn along NE–SW direction to constrain the along axis depth variations (Figure 3 a–f). The various tectonic elements of the TF, viz. tectonized zone, principal transform displacement zone and the transform azimuth from trends of the transform valleys have been estimated.

Results and interpretations

We have mapped in detail for the first time the three major areas of TF–SL, VT and VM and also the TF #4 (named as Ehrlich) just north of the VM TF. The results and interpretations of the multi-beam data presented here are based on an observation of large-scale maps with contour intervals of 50 m.

Morphotectonics

The study region, spanning between 3°S and 10°S along and around the CIR, is characterized by seven short ridge segments, dislocated right-laterally by 6 long offsets caused by FZ and TF. The depth of the seafloor, including that along the axial valley, FZ valley and outer flanks, ranges from 1500 m to 6500 m. We describe the morphotectonics of studied regions under three categories: ridge axial valley, ridge-TF intersection and FZ (RTI + FZ) and outer flanks.

Ridge axial valley: The northernmost major TF, dislocating the CIR, is the SL TF and the studied region encompasses ridge segments IX and VIII located between

3°S to 4°40'S. Detailed bathymetry data along six profiles in a NE–SW direction were acquired in VM area, of which two profiles ran across the northern ridge segment (#IX), another three profiles across the southern ridge segment (VIII), while one profile (Figure 3 a) partially ran along the SL TF. The ridge axial valley prominently displays a W-shape, with northeastern shoulders in both the segments rising to lesser height than the southwestern one. In addition, there have been at least two minor left-lateral displacements ranging from 1.5 to 2 km of the valley floor within the northern ridge segment (second order discontinuity). Compared to the northern segment, the depth of the valley floor in the southern segment is overall shallower and never reached deeper than 4000 m. However, in both the segments, the depth of the valley floor increases towards RTI.

The second major transform mapped was VT TF and the ridge segments VI and VII between 4°40'S and 6°45'S. Bathymetry and geophysical data were collected along seven profiles across the northern segment VII and another six across the southern segment VI. Data along one long profile over the VT TF/ FZ and another three short profiles across the VT TF were collected. The results show several interesting morphotectonic features. For example in the northern segment, the axial valley varies in width between 7 km close to the RTI to about 18 km at the central part, in contrast to widening of the valley floor at RTI. The depth of the valley floor however, increases from 3500 m at the central region to more than 4500 m near the RTI. About 20 km to the north of the VT TF, the axial valley floor seems to have been locally dislocated right-laterally by a minor TF by about 13 km (2nd order discontinuity). This dislocated area seems to be occupied by a pronounced seamount that rises to ~2000 m from the valley floor. The axial valley along the southern segment of VT area is much shallower (less than 3250 m) compared to the northern segment and lacks any definite flanks. This shallowness of the axial valley between 5°40'S and 6°15'S is comparable to the characteristics of fast spreading ridge and is strikingly different to segments north of the CIR.

Table 1. Details of sampling carried out along the NCIR during SK #165. D, depth; DG, Dredge; BA, Biomass; SC, Sediment core; ADCP, Acoustic Doppler Current Profiler

Station	Lat. (°S)	Long. (°E)	D (m)	Topography	Recovery	Remarks
9DG	9 53.64	66 35.72	2000	Seamount, west of ridge axis	Massive and fragments of columnar and pillow basalts from summit	West of segment III, north of TF 2, near-axis seamount
	9 53.10	66 6.77	1875			
10BA	9 50.08	66 41.95	2500	–	Biomass + ADCP	Segment III, along the axial valley
15SC	8 27.56	67 39.41	2810	Patches of thick sediment	Little recovery of siliceous clay	West of segment IV, north of TF 3
18BA	8 18.60	67 56.90	2120	On seamount flank	Biomass + ADCP	West of segment IV, north of TF 3
20BA	8 12.11	68 7.98	2630	–	Biomass collected	Axial valley of segment IV
22DG	6 02.30	6 17.66	2370	Smooth up slope of 800 m	Small amount of calcareous sediment	East of segment VI, South of TF 6
	6 03.43	68 14.8	2100			
24DG	5 29.75	68 13.42	2470	Seamount with steep slope	15 rock pieces	Far west of segment VII, north of TF 6
	5 31.99	68 12.03	2050			

The third major FZ-influenced region studied has been around VM TF extending between 7°40'S and 10°40'S. The width of the ridge axial valley of the northern segment (#IV) increases from 12 km at the central portion to 17 km at the intersection with VM TF. Similarly, the depth of the axial valley floor increases from about 3000 m at the centre of the segment to more than 4000 m at the RTI. The shape of the axial valley in the southern segment (#III), south of VM TF, takes an 'I'-design, with a relatively narrow valley floor at the central portion (24 km) bordered by wide valley at the south (30 km) and at the north (35 km). The depth of the axial valley floor has been registered between 3500 m and 3700 m with indication of deepening towards the RTI.

Ridge-transform fault intersection and fracture zone (FZ). The NE-SW trending SL TF has dislocated the northern and southern ridge segments right-laterally by about 55 km. The RTI in VM area is deeper (> 4500 m) at the intersection of southern segment and the FZ (Figure 3 a) than that in the intersection of northern segment with the SL TF (little more than 4200 m). The width of the transform flanks has been more than 8 km. Close to the western RTI within the transform valley, locally an elevated horst type topography is noted. The summit area of this feature is about 5 km², ellipsoidal in shape and oriented parallel to the FZ.

The NE-SW trending VT FZ dislocated the northern and southern CIR ridge segments right-laterally by about

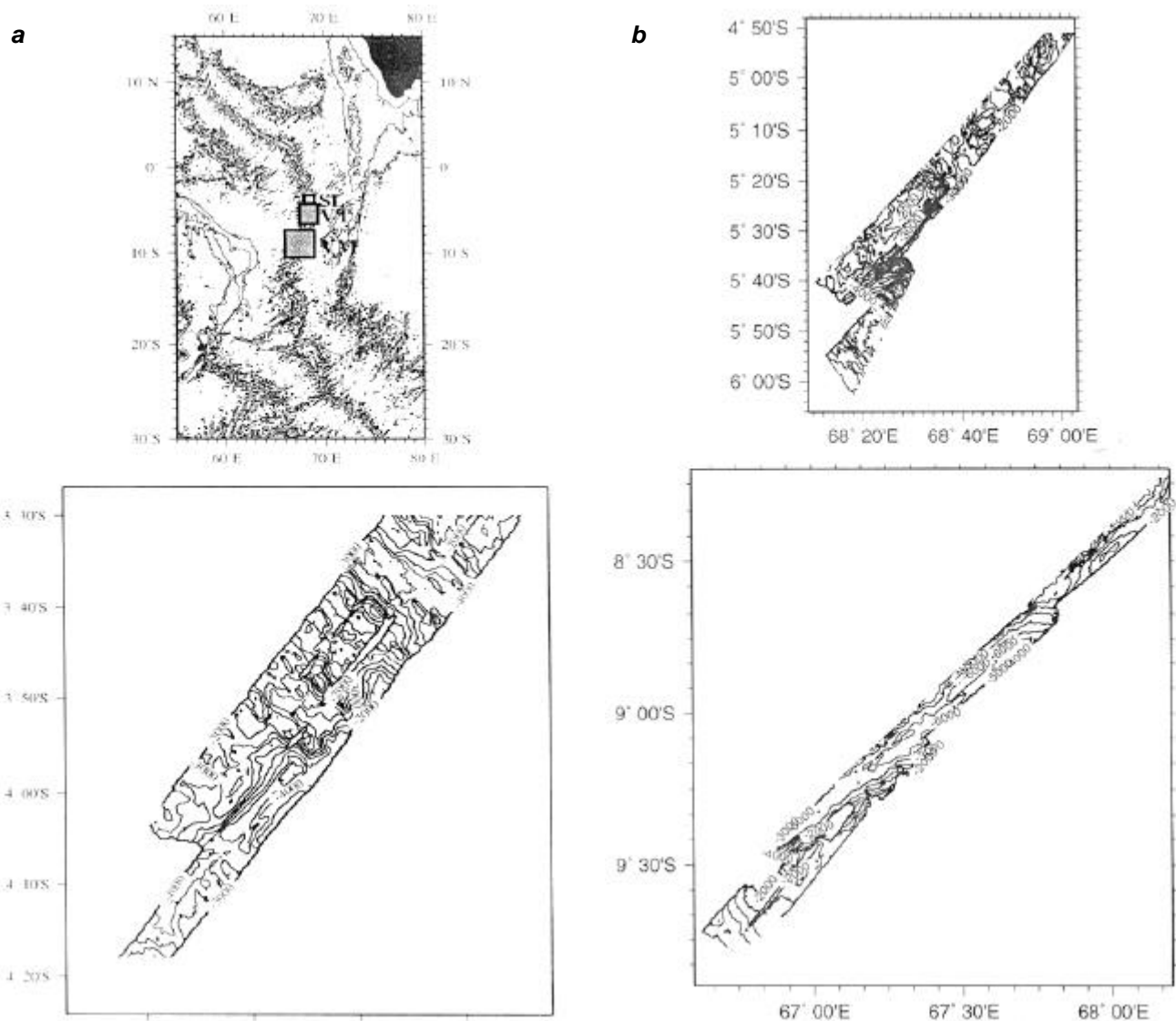


Figure 2. *a*, Multi-beam bathymetric maps of the studied regions. The top panel shows the general features of the CIR with the location of the study areas and the bottom panel shows VM area. Contour interval = 500 m. *b*, The upper and lower panels depict the VT and VM regions, respectively. Contour interval = 500 m.

94 km. The width of the transform valley attains to approximately 10 km (Figure 3 a) and the depth varies from 3000 m along the flanks to > 5000 m at the centre. The valley floor is devoid of any prominent features, except for some localized circular to lenticular deeper areas.

The TF #4 (Ehrlich TF), north of the VM TF, was mapped through along, over and across profiles. The survey reveals a complex morphotectonic character comprising alternating troughs (4800 m deep) and crests (2300 m) suggestive of intense deformation. The deepest RTI was found here (> 6100 m, Figure 3 b) and deserves further detailed investigations. Figure 3 b (bottom curve) shows the along axis depth variation in ridge segment #IV with valley floor deepening to a depth of > 5100 m at the segment centre which shallows northward to a depth of 3500 m.

The VM FZ has dislocated the NCIR by about 344 km. The width and depth of the floor of the transform zone has been 12 km and 3000–4000 m on the east respectively, which increased towards the central portion of the FZ (> 6000 m) and then reduced again towards the west (Figure 3 c profiles VM10, VM16). The floor of the cen-

tral part of the NE–SW trending VM TF is flanked on the inner side by crenulated and elevated topography. The VM FZ is one of the prominent features in the Indian Ocean, as it hosts the deepest point on the seafloor in this ocean. The present survey has mapped this point, which reaches beyond 6500 m. The deepest area records a width of about 5 km and length of 12 km. A recent bathymetry survey of this area reveals the presence of slip movement at local scale along the floor of the VM TF (J. Leven, pers. commun.). Although it is difficult to comprehend the origin of the deepest area based on the data available presently, the possibility of the deepest part representing a graben structure caused by local dip-slip movement cannot be ruled out.

Outer flanks: In SL area a number of ridge parallel ridges, hills and seamounts occur. The western outer flanks of the northern segment records four CIR parallel ridges within 40 km from the axial valley, at an average spacing of 9.5 km. These ridges rise in height from 2200 m to as shallow as < 1800 m. In contrast, there are very few not-so-prominent ridges located on the eastern

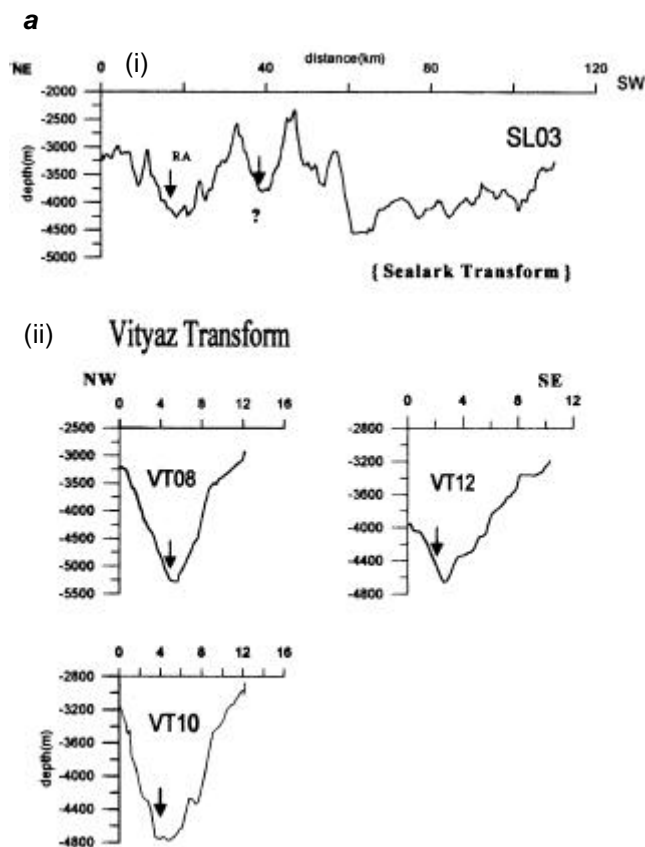


Figure 3 a. (i) Profile along SL TF. The profile on the left is across the ridge axis whereas towards the right is along the SL TF. Arrow indicates location of the ridge axis. (ii) Profiles across VT TF in the NW–SE direction. Depth varies from 4600 to 5300 m. Valleys are generally ‘V’-shaped except in one case (VT 10) where a hump is present on the valley floor. Arrows indicate the location of the axis of transform valley.

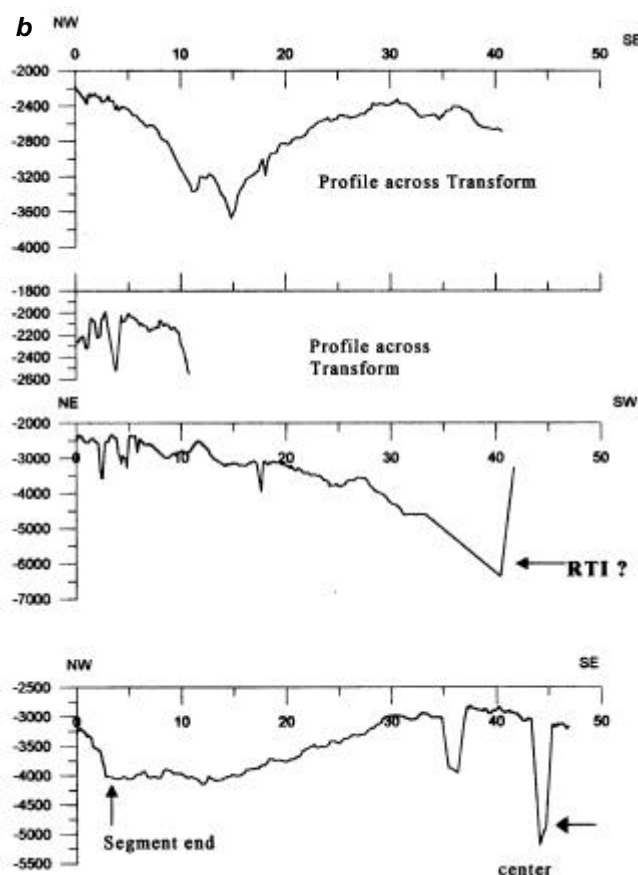


Figure 3 b. Profiles across and along Ehrlich TF. The third profile, along transform, depicts the deepest point (6000 m) near the ridge axis (Ridge-Transform Intersection). The bottom profile is along the ridge segment IV, indicating deepening (5189 m) at the segment centre and shallowing towards the northern segment end.

outer flanks of the northern segment, rising in height not shallower to 2000 m. This may have resulted from the asymmetric nature of spreading, as indicated by minor left-lateral displacements of the axial valley as described earlier. On the other hand, in the southern segment of SL area, four segment parallel ridges are located on the western flank within 53 km from the axial valley at a spacing between 11 and 19 km. The heights of these ridges shallow from 2600 m close to the FZ (profile SL04) to < 1800 m away from the FZ influence (profile SL06). On the eastern flank, the ridges are largely faint in expression rising only to 400–600 m from the seafloor depth of approximately 3000 m. However, along profile SL05, few shallower ridges are found at a spacing of 8 km of more than 1000 m in height.

In VT area, two ridges (height < 2000 m) occur on the eastern flanks of the northern segment. The first one, a CIR-normal ridge, is located about 19 km from the axial valley (summit dimension ~ 15 km²), while the other ridge trends parallel to the CIR axis (summit dimension ~ 27 km²) and occurs about 51 km from the axial valley. Ridges of similar types also occur on the western side of the northern segment where on the top of a single, broad, elevated plateau, two prominently peaked ridges occur—a NE–SW trending ridge (height < 2000 m, summit dimension 207 km²) at about 16 km from the axial valley, while the other NW–SE oriented (summit dimension ~ 43 km²) ridge occur at a distance of about 39 km from the axial valley. On either flanks of the southern segment, spreading ridge parallel ridges (height < 2000 m) are pre-

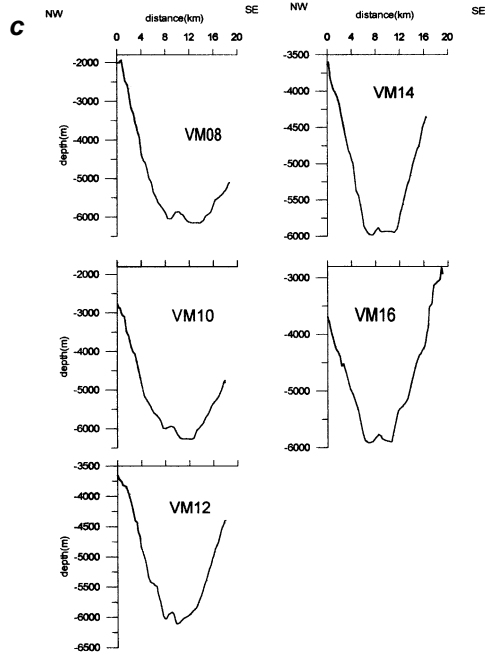


Figure 3 c. Profiles (NW–SE) across VM TF from NE to SW flank. Depth mainly varies from 6000 to 6200 m (avg. 6000 m). Small humps on the axial valley floor could represent neo-volcanic zone. The arrows indicate the location of the axis of transform valley zone.

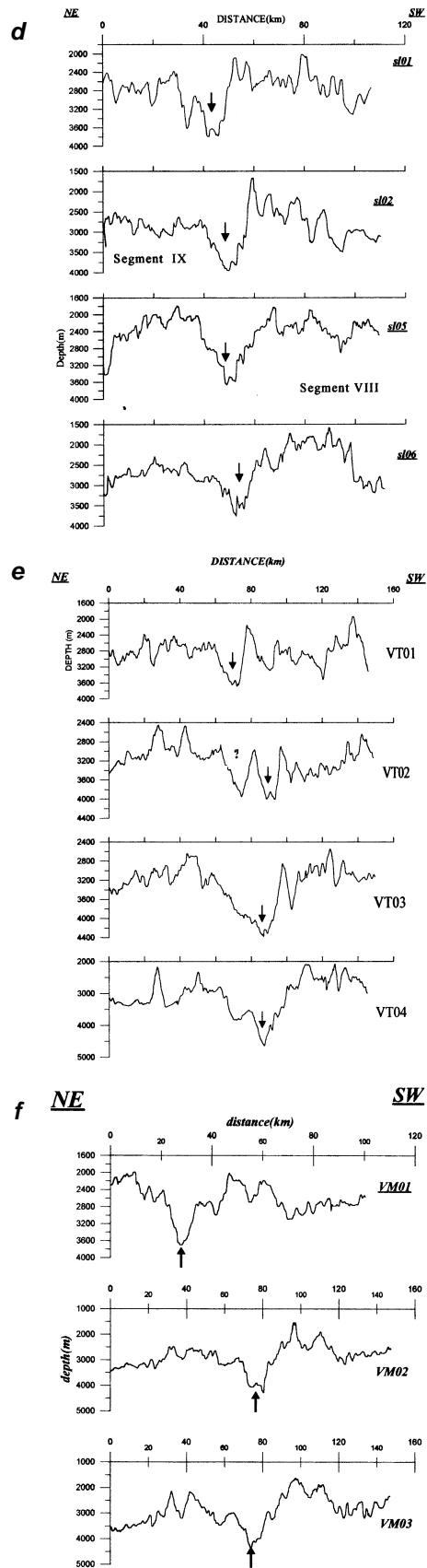


Figure 3 d–f. Profiles across the Sealark, Vityaz and Vema ridge segments respectively.

sent at a distance of about 15 km, 49 km, and 58 km from the axial valley.

In the spreading ridge segment immediate north to the VM FZ, the outer flanks of the axial valley reveal the presence of several ridge parallel elevations, the first one at about 5 km (elongated in NW-SE direction) and the other is nearly circular at 6.5 km east of the axial valley. On to the west, a seamount occurs at about 5 km of the axial ridge. In addition, the overall seafloor to the west of the axial valley is quite elevated. All these elevations rise to a height of < 2000 m from a general seafloor depth in excess of 4000 m. The western outer flank of the southern segment is characterized by the striking presence of a shear zone. About 96 km long, this shear plane broadly separates the shallower northern part (2000 m) and relatively deeper southern part (> 3000 m). Interestingly, this shear plane does not extend to the eastern part cutting across the ridge axis and there have been volcanic eruptions at least in two places. The seamount occurring at about 90 km west of the axial valley is largely circular in shape, with basal dimension 24 km². At this seamount, two types of basalts were found – pillow and columnar, suggesting two episodes of volcanic eruptions. The magnetic studies over this seamount also suggest the effect of overprint magnetization⁵ (details in petrology section). Another small seamount occurs about 124 km west of the axial valley.

Magnetics

We have identified magnetic anomalies up to three across ridge segments III to IX on various profiles in the three regions (Figure 1). While the median valley is typified by broad amplitude anomaly of 200–400 nT, anomalies associated with FZ are relatively subdued and < 200 nT across the deepest part of Vema FZ.

The three critical parameters, viz. distribution of earthquake epicentres, central anomaly magnetic high (CAMH) and associated negative free-air anomaly (satellite derived and ship-borne) have been used to constrain the location of the ridge-axis in the study area in conjunction with available multi-beam and single-beam bathymetric data. The other parameters used are morphologic signature of an active volcanic ridge and axial zone of high seafloor reflectivity. The CAMH occurs over the zone of most recent volcanism in some segments whereas most of the CAMH locations picked on magnetic profiles correspond to axial bathymetric valley. The earthquake events are quite well correlated to the bathymetric trends of the spreading segments.

By considering the spreading rate, which records the motion between Africa/India and Africa–Australia plates since the time of anomaly 3, we have computed the flank spreading rates after matching the observed anomaly shape with the synthetic one. The mean half-spreading

rate of 18 mm/yr in the SL and VT regions increases to 21 mm/yr south of the VM TF. The nature of intra- and inter-segmental variations in magnetic anomalies suggests that the region between south of VT and north of VM is likely to have distinct signatures of Africa–India/Africa–Australia plate motion, which could possibly be due to an evolving triple junction in this region, as also attested by the bathymetry. For example, the axial valley along the southern segment of VT area is much shallower (less than 3250 m) compared to the northern segment and lacks any definite flanks. This shallowness of the axial valley between 5°40'S and 6°15'S is comparable to the characteristics of fast-spreading ridge and is in contrast to that of northern segments of CIR.

Petrology

The rocks collected from two near-axis seamounts (samples #9DG and 24DG, Table 1) are distinct in type and texture. From the seamount (summit height 1875 m) in VM area (west of segment #III), a near dredge-full of columnar and few pillow basalts were recovered (Figure 4 a). The recovery of columnar basalts (#9DG) is quite significant as these plausibly suggest a special regime of eruption and consolidation of the lava. The columns are either cylindrical or conical and have glassy veneer on top. The individual columns are 1–4 cm wide and 3–40 cm long. Vesicles are commonly present at the sides of the column. Some samples show a discontinuous cover of ferromanganese coating. Few cross-sections of the columns have a chilled glassy margin of 3–4 mm thick at the top, followed by a fresh basaltic interior, consisting of plagioclase (4–20%), olivine (0.7–2%) and a few pyroxene in the groundmass.

The morphology of plagioclase (phenocryst/ micro-phenocryst/zoned/belt buckle/acicular/sheaf like) (Figure 4 b, c) may result from variation in depth of magma generation, degrees of cooling and rate of crystal separation. The abundance of olivine is nearly proportional to that of pyroxene up to a certain extent beyond which both plagioclase and olivine reduce and pyroxene increases. Numerous spherical melt inclusions within the plagioclase attest to their post-entrapment crystallization (Figure 4 d). The dominance of amphibole (mainly replacing the clinopyroxene) in the columnar basalts plausibly suggest hydrothermal alteration of the basalts. The other near-axis seamount (summit height 2050 m), dredged to the west of ridge segment #VII in VT area (sample #24DG) has aphyric to sparsely phyric basalts with 2–3% plagioclase and altered glass.

Of the opaque minerals, magnetite is ubiquitous as titanomagnetite (TiO₂ 18–39%, Fe₂O₃ 71–77% by EDS analysis) and occurs as aggregates of subhedral to anhedral grains. Magnetite also occurs as skeletal crystals, thin lamellae, globular to subglobular clots throughout the

groundmass and as tabular crystals parallel to the plagioclase twin lamellae, euhedral grains being rather sporadic. The rare presence of crystals of chromite (Cr_2O_3 , 97%) has also been noted in these basalts.

It is noteworthy that based on the geophysical data acquired during cruise #125 near the sample 9DG, Drolia *et al.*⁵ hypothesized the possibility of overprint magnetization. According to these authors, the rocks near the TF were demagnetized when the thermal anomaly associated with the ridge axis in segment #II passed close to the area (segment #III) and remagnetized when the rocks cooled again below their Curie temperature. The samples from 9DG seem to provide some clue to support the above view by hinting at two lava eruptions in the past. The first eruption probably formed pillow basalts while during the second eruption, basaltic dikes formed below the pillows and this on cooling produced the columnar basalts. This kind of feature has been sometimes noted at the MOR¹⁴. The presence of two types of basalts may thus, help explain the rise and fall of temperature across the Curie point and consequently the observed overprint magnetization of the oceanic crust.

The manganese nodules with low Mn/Fe ratio (< 1) and low Cu and Ni contents than those from basinal regions indicate their possible hydrothermal–hydrogenous origin. The TF appear to have acted as conduits for movement of nutrient-rich water masses from Somali to the Arabian basin and in the process enhanced the growth of nodules. The concentration of lighter boron isotopes (av. 38‰) in the upper 300 m layer of the seawater and the heavier isotopes (av. 39‰) below this depth indicate that concentration of $d^{11}\text{B}$ vary along the water column⁶.

Near VT a 15-cm thick carbonate substrate encrusted with ferromanganese oxides was recovered. The calcareous nannoplankton assemblage indicates the infringement of the oxygen minimum zone during the deposition of the carbonates. The hiatuses present in the western Indian ocean probably resulted due to the prevalence of intermediate subsurface currents¹⁵.

Biological studies

Biological samples were recovered to study the MOR inhabitants. Marine organisms (jelly-fish, brittle star, etc.)

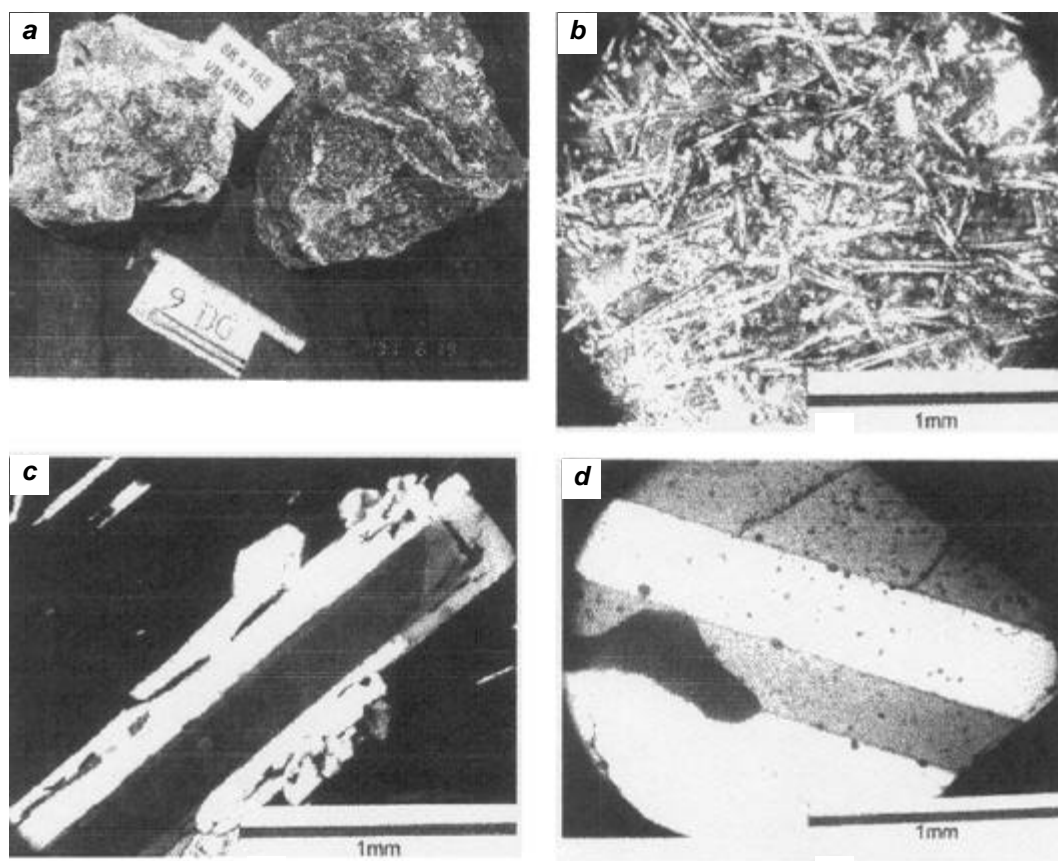


Figure 4. *a*, Two of the largest basalt specimens recovered at station 9DG. Sample on the left is massive with glassy margin on top and the sample to the right has columnar features. *b*, Photomicrograph of basalt showing acicular quenched grains of plagioclase with dendritic projections (plane light, $\times 50$). *c*, Photomicrograph showing the well-developed zones in plagioclase phenocrysts (crossed nicols, $\times 50$). *d*, Photomicrograph depicting globular melt inclusions in plagioclase with straight lamellar twinning (crossed nicols, $\times 50$).

that came in the dredge were preserved in 10% formalin. The total biomass was collected using a Bongo net with 300 µm mesh size and the retrieved samples were stored in 5% formalin for further analysis. Studies are underway of the collected fauna.

Conclusions

- Along-axis depth variations were noted with deepening at segment ends and shallowing at segment centers (VT and VM regions). The deepest RTI has been mapped at the Ehrlich Transform-Ridge Segment IV intersection.
- Magnetic anomalies along the northern profiles across the ridge indicate the axis to be an active spreading centre. The magnetic anomaly was traced up to 3A.
- Fresh to slightly altered basalts (pillows and columns) were recovered. In VT area, the basalts form substrates and nuclei for accretion of ferromanganese oxides.
- A deep central plumbing system, fed by distinctive mantle sources, may have supplied magma as uprising diapirs to several small discontinuous buoyant chambers situated at shallow depths along the ridge crest or else the melt surfaced through multiple dyke injections.
- Calcareous nannoplankton of early Pliocene age in the vicinity of VT suggests a change in the depositional environment around the time when large depositional hiatuses occurred¹⁵.

1. Sandwell, D.T. and Smith, W. H. F., Marine gravity anomaly from Geosat and ERS 1 satellite altimetry. *J. Geophys. Res.*, 1997, **102**, 10,039–10,054.
2. DeMets, C., Gordon, R. G. and Vogt, P., Location of the Africa–Australia–India triple junction and motion between the Australian and Indian Plates: results from an aeromagnetic investigation of the central Indian and Carlsberg ridges. *Geophys. J. Int.*, 1994, **119**, 893–930.
3. Chaubey, A. K., Krishna, K. S., Subba Raju, L.V. and Rao, D.G., Magnetic anomalies across the southern Central Indian ridge: evidence for a new transform fault. *Deep-Sea Res.*, 1990, **37**, 647–656.
4. Kamesh Raju, K. A., Ramprasad, T. and Subrahmanyam, C., Geo-

physical investigations over a segment of the Central Indian Ridge, Indian Ocean. *Geo-Mar. Lett.*, 1997, **17**, 195–201.

5. Drolia, R. K., Ghose, I., Subramanyam, A. S., Malleswara Rao, M. M., Kessarkar, P. and Murthy, K. S. R., Magnetic and bathymetric investigations over the Vema region of the Central Indian Ridge: Tectonic implications. *Mar. Geol.*, 2000, **167**, 413–423.
6. Mukhopadhyay, R., Murthy, K. S. R., Iyer, S. D., Malleswara Rao, M. M., Banerjee, R., Subramanyam, A. S., Shirodkar, P. V. and Ghose, I., InRidge Program: Preliminary results from the first cruise. *Curr. Sci.*, 1998, **75**, 1157–1161.
7. Drolia, R. K., Iyer, S. D., Chakraborty, B., Kodagali, V. N., Mukhopadhyay, R., Nanyasi, S. K., Sarma, K. V. L. N. S., Rajasekhar, R. P., Misra, S., Ray, D., Andrade, R., Lasitha, S., Varghese, J., Jacob, J., Sukumaran, N. P., Pednekar, A., Furtado, R. and Nair, A., Preliminary results of a recent cruise to the Northern Central Indian Ridge. *InterRidge News*, 2002, **11**, 43–46.
8. Kalyayev, G. I., Karabovich, S. V., Rusakov, O. M. and Startostenkov, V. I., Deep structure of the Arabian–Indian Ridge and the Owen fault zone. *Geotectonics*, 1983, **17**, 32–42.
9. Herzig, P. M and Plüger, W. I., Exploration for hydrothermal activity near the Rodriguez triple junction. *Indian Ocean. Canad. Mineral.*, 1988, **26**, 721–736.
10. Mukhopadhyay, R and Iyer, S. D., Petrology of tectonically segmented Central Indian Ridge. *Curr. Sci.*, 1993, **65**, 623–628.
11. Plüger, W. L., Fahrtbericht SO 28 and Wissenschaftlicher Bericht GEMINO I: Geothermal Metallogenesis Indian Ocean. 1988.
12. Cande, S. C. and Kent, D. V., Revised calibration of the geomorphological polarity time scale for the late Cretaceous and Cenozoic. *J. Geophys. Res.*, 1995, **100**, 6093–6095.
13. Anon, Cruise Report ORV Sagar Kanya Cruise 165, 2001, p. 39.
14. McBirney, A. R., Oceanic Volcanism: A Review. *Rev. Geophys. Space Phys.*, 1971, **9**, 523–556.
15. Guptha, M. V. S., Banerjee, R. and Mergulhao, L., On the nature of calcareous substrate of ferromanganese crust from the Vityaz fracture zone. *Geo-Mar. Lett.*, 2002, **22**, 12–18.

ACKNOWLEDGEMENTS. We acknowledge the Office of Naval Research, USA, for funding this project for the period 1997–2004. RKD was partly funded by the Department of Science & Technology, New Delhi. We thank the Department of Ocean Development, New Delhi, for the availability of *ORV Sagar Kanya* and Dr M. Sudhakar, National Centre for Antarctic and Ocean Research (NCAOR), Goa, for allotting the cruise as scheduled and for the logistics. We are obliged to Dr E. Desa (Director, NIO), Dr P. C. Pandey (Director, NCAOR) and Dr V. P. Dimri (Director, NGRI) for constant encouragements. M. V. Ramana, K. Srinivas, V. Khedekar, A. Y. Mahale (all from the NIO) and Dr P. Dasgupta (Presidency College, Kolkata) lent timely help. We appreciate the critical suggestions provided by the reviewer. The Captain, officers, crew, participants and engineers of Norinco Pvt Ltd., extended their cooperation during the cruise. NIO's contribution # 3831.